

ORIGINAL ARTICLE

Theoretical Study of Water Dissociation on Aluminum (100) Surface using Density Functional Theory

| Dimbimalala, Randrianasoloharisoa ^{1*} | Herimanampisoa, Randrianarinjaka ¹ | and | Georgette, Ramanantsizehena ¹ |

¹ Université d'Antananarivo | Département de Physique | Laboratoire de Physique de la Matière et du Rayonnement | Antananarivo | et Madagascar |



| DOI: 10.5281/zenodo.13354320 | | Received July 19, 2024 | | Accepted August 21, 2024 | | Published August 24, 2024 | | ID Article | Dimbimalala-Ref07-2-19ajiras190824 |

ABSTRACT

Background: The background is well-stated and accurately describes aluminum as a widely abundant, metallic catalyst used in heterogeneous catalysis applications. **Objectives:** The objectives are clearly defined and focused on the theoretical study of water (H₂O) adsorption and dissociation on the (100) surface of a cubic, face-centered aluminum (Al) structure. **Methods:** The methods section provides a comprehensive overview of the computational approach used in this study. The details about the use of density functional theory (DFT), the Dacapo code, and the Nudged Elastic Band (NEB) method for determining the reaction pathway are all clearly explained. **Results:** The results section summarizes the key findings of the study, including the adsorption energies for H₂O, H, and OH, as well as the calculated energy barrier for the dissociation of H₂O into H+OH on the Al(100) surface. **Conclusions:** The conclusions drawn from the results are reasonable and well-supported. The authors highlight the stability of the dissociatively adsorbed H and OH species compared to the molecularly adsorbed H₂O, suggesting the feasibility of water dissociation on the Al(100) surface. However, the authors also note the relatively high energy barrier for the dissociation process, which could indicate the need to explore alternative reaction pathways or the use of aluminum alloys.

Keywords: density functional theory, DACAPO, Nudged Elastic Band, water, aluminum, adsorption, dissociation.

1. INTRODUCTION

Catalysis is a crucial field of research, with significant implications for various industries such as petrochemicals, agri-food, and pharmaceuticals. Over 90% of industrial chemical products are manufactured with the aid of catalysts [1,2]. The study of catalytic materials and their properties has become a strategic area of focus, as there is a growing demand for efficient processes that can minimize synthesis steps while maximizing productivity. Adsorption, a surface phenomenon whereby gas or liquid molecules adhere to the solid surfaces of adsorbents, is a fundamental aspect of many catalytic processes. Two distinct types of adsorption are recognized: physical adsorption (physisorption), where the bonds are weak and the interactions are dominated by van der Waals forces, and chemical adsorption (chemisorption), in which the gas molecules and the substrate form covalent or ionic bonds, creating new chemical species on the surface [3].

The dissociation of water (H₂O) molecules on metal surfaces is a critical process in various applications, such as hydrogen production and fuel cell technologies. Hydrogen is a promising alternative fuel, as its combustion with oxygen produces water as the only byproduct, making it a clean and sustainable energy source. However, the dissociation of water molecules on catalytic surfaces is a complex process that requires a deeper understanding of the underlying mechanisms. Aluminum (Al) is a widely abundant, inexpensive, and relatively non-toxic metallic element that has been explored for its potential in heterogeneous catalytic applications [4]. This work aims to contribute to the understanding of the physical and chemical properties of the free H₂O molecule, the adsorbed H atom, the free OH fragment, and the adsorbed OH species on the Al(100) flat surface. The adsorbate-surface interactions and the reaction process of H₂O dissociation will be studied using ab initio methods based on density functional theory (DFT), specifically the Dacapo code (Danish ab initio pseudopotential code), which employs pseudopotential approximation and a plane-wave basis set.

2. MATERIALS AND METHODS

2.1 Computational method

In this work, we utilized the Dacapo program grounded in Density Functional Theory (DFT) employing a plane wave basis set [5,6]. The ionic cores are simulated by using ultrasoft pseudopotentials developed by Vanderbilt (1990) [7]. The self-consistent solution of the Kohn-Sham one-electron equations was pursued, employing GGA functional parameterized by Perdew-Wang (GGA-PW91) for the exchange-correlation part [8,9]. Geometry optimization was conducted by using the BFGS method and all forces are calculated by using the Feynman theorem (1939) [10]. Brillouin zone sampling utilized generation of k-points using the Monkhorst and Pack method (1976) [11]. In our calculations, the force gradient threshold must be less than or equal to 0.05 eV/Å.

The important two parameters left to determine to carry out the simulation are the cutoff energy, which is proportional to the number of plane waves used to develop the system's Hamiltonian, and the number of k-points used. The cutoff energy must be sufficient to accurately represent the electronic system and ensure good total energy precision. In the case of transition metals, Baraldi et al., (2004) [12] suggested that a cutoff energy of 340eV is sufficient. Since this value depends

on the chemical species used in the calculations, in this work, we considered a cutoff energy of 350 eV. Next, determining the k-point density is necessary for the convergence of the total energy of the system. The higher this density, the better the precision in the calculations, but the calculation time becomes much longer. For a (2x2) cell of Ni(111), Haroun (2007) [13] estimated a k-point density of (5x5x1). The same result was found by Moussounda (2006) [14] in his study on a (2x2) cell of Pt(100). Thus, we also chose the same k-point density (5x5x1) for all the calculations in this work.

2.2 Parameters related to the supercell

Since the DACAPO code is based on DFT, plane waves, and pseudopotentials, it requires a system invariant by translation according to Bloch's theorem. In the case of a surface, where translation invariance is no longer respected along the (Oz) direction, it is necessary to insert empty space to preserve 3D periodicity for study in space. The system to be studied is then represented by the repetition of a supercell, as shown in figure 1, containing a finite number of atomic planes, called slab, and empty space. The system becomes periodic by translation in all three directions, but the height of the empty space and the thickness of the slab are two important parameters in the calculations.

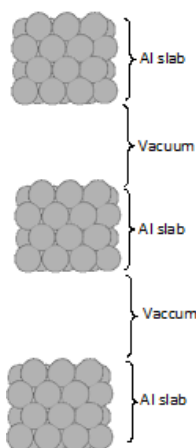


Figure 1: The figure shows the principle of supercell.

To form the slab, the number of atomic planes is chosen so that the interaction between the two faces of the slab is negligible. Here, the slab consists of stacking Al(100) planes along the (Oz) direction. The minimum thickness of this slab is determined by increasing the number of planes while keeping the height of the vacuum constant until the variation of the total energy per layer equals the cohesion energy of the crystal. This allowed us to take a slab of four layers for our calculation. The empty space separating two successive slabs must be wide enough so that the interactions between the slabs become negligible. However, calculations involving a large cell size take longer. Therefore, a compromise is sought between canceling interactions and calculation time. For this reason, Haroun (2007) [13] suggested that the minimum slab-slab (vacuum) distance is 10 Å to eliminate this interaction. In this work, we chose a vacuum space distance of 12 Å.

2.3 Construction of the surface

In this work, we used a (2x2) lattice of the (100) plane of Al, as shown in figure 2. The choice of this cell is motivated by the enlargement of the adsorption surface of the H₂O molecule compared to a (1x1) lattice of aluminum.

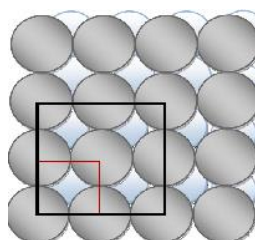


Figure 2: The figure represents a (2x2) surface of Al(100) (black square) and a (2x2) surface (red square).

2.4 Adsorption of H₂O

By convention, the adsorption energy of a H₂O molecule is defined by:

$$E_{ads} = E_{H_2O/Al} - [E_{H_2O} + E_{Al}] \quad (1)$$

Where:

$E_{H_2O/Al}$ represents the total energy of the {H₂O + Al} system,

E_{H_2O} is the total energy of the isolated H₂O molecule,

E_{Al} is the total energy of the isolated slab, i.e. Al substrate.

According to this definition, it should be noted that the negative value of the adsorption energy corresponds to a stable situation of the $\{H_2O + Al\}$ ensemble.

2.5 Co-adsorption of OH and H on Al(100) surface

The OH and H fragments jointly adsorbed on the Al(100) surface represent the final state of water molecule dissociation into H and OH. Using the same convention as in the previous case for the calculation of adsorption energy, we can write:

$$E_{ads} = E_{(OH+H)/Al} - [E_{H_2O} + E_{Al}] \quad (2)$$

Where:

$E_{(OH+H)/Al}$: represents the total energy of the $\{(OH+H) + Al\}$ system,

E_{H_2O} : is the total energy of the isolated H_2O molecule,

E_{Al} : is the total energy of the isolated slab, i.e. Al substrate.

2.6 NEB Method

The NEB (Nudged Elastic Band) method [15] aims to obtain a certain number of intermediate images of the water molecule along the reaction path. Each image evolves towards an optimal configuration, i.e., each image is relaxed to be in the state with the lowest possible energy while remaining equidistant from neighboring images. The NEB method allows to determine the activation energy, i.e. the energy necessary to pass the energy barrier to go from a stable configuration to another. To implement the NEB method for the dissociation reaction of the water molecule on the Al(100) surface, it is necessary to define the initial and final states of the dissociation: The initial state is represented by the state of the H_2O molecule in the gas phase adsorbed on the Al(100) surface, while the final state is the state of the system where the OH and H fragments are coadsorbed on the surface. The NEB program can then be set in motion to reproduce the reaction pathway, going from the initial state to the final state, i.e., the transition from $H_2O/Al(100)$ to $(OH+H)/Al(100)$. The N configurations required to transition from the initial configuration to the final configuration are calculated ab initio for each, with geometric relaxations of the adsorbed molecule and the first plane of Al. We fixed number of configurations set to 10, including the initial and final states.

3. RESULTS AND DISCUSSION

3.1 Lattice parameter of aluminum

Aluminum is a metal with a face-centered cubic (fcc) crystallographic structure. To determine the lattice parameter, we consider a three-dimensional crystal of aluminum. We calculate the energy of the unit cell for different parameter values to identify the value that would minimize this energy. According to the simulation, the minimum energy corresponds to a crystal parameter of 4.045 Å. This value is very close to that found by Witt (1967) which is 4.049 Å. [16]

3.2 Adsorption of H_2O

3.2.1 Geometric structures and adsorption energy: Before performing adsorption of H_2O on Al(100) surface, we begun by considering the characteristics of isolated H_2O molecule. Distances between oxygen atom with each hydrogen atom denoted H(1) and H(2) are the same and equal to 0.978 Å. Distance between the two hydrogen H(1) and H(2) is equal to 1.548 Å and the H-O-H angle is 104.51°. The shape of the H_2O molecule obtained is depicted in figure 3.

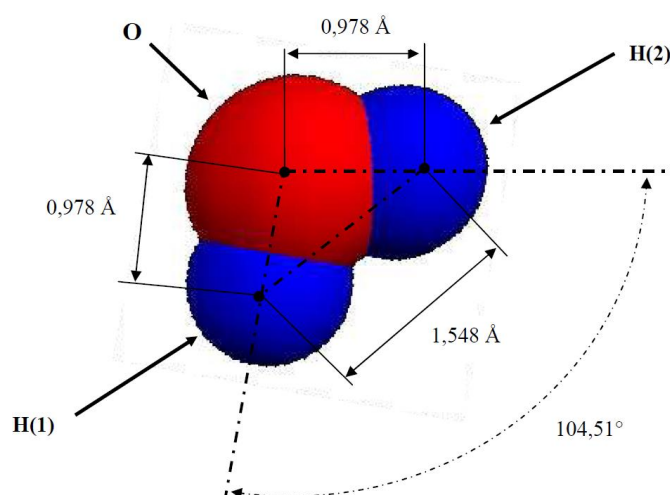


Figure 3: The figure presents geometric characteristics of a H_2O molecule

Other several studies have been conducted to obtain characteristics of H₂O molecule. The work of Hoy and Bunker (1979) provided the experimental value for the distance between the oxygen atom O and one of the hydrogen atoms H, denoted as O-H, which is 0.959 Å, and the H-O-H angle, which is 105° [17]. Giuliana Materzanin et al., (2005) obtained theoretical values of 0.972 Å for the O-H distance and 105.2° for the H-O-H angle [18]. Xantheas and Dunning (1993) found 0.959 Å and 104.3° [19]. Finally, Rakotvelo (2008) found values of 0.980 Å and 104.3° [20].

Table 1 summarizes our calculation results compared with those of others authors.

Table 1: This table shows the values obtained in this work with those of other researchers.

	Hoy et al., (1979) [17]	Giuliana et al., (2005) [18]	Xantheas et al., (1993) [19]	Rakotvelo (2008) [20]	Our results
Distance O-H (Å)	0.959	0.972	0.959	0.980	0.978
Angle H-O-H (°)	105	105.2	104.3	104.3	104.51

We observe that the results obtained are in good agreement with these values. For the distance O-H, the deviation observed from the experimental value of Hoy et al., (1979) is 1.9%, it is 0.6% compared to the results of Giuliana et al., (2005), 1.9% compared to Xantheas et al., (1993), and 0.2% compared to results of Rakotvelo (2008) [17,18,19,20].

The total energy of the H₂O molecule obtained is E_{H₂O} = -469.523 eV. We notice that the result obtained for the energy is in good agreement with that found by Rakotvelo (2008) which is -469.533 eV [20]. The calculated energy of clean Al surface is E_{Al} = -900.126 eV and the energy of H₂O/Al system is E_{H₂O/Al} = -1369.915 eV. From this value of energies, we calculated the adsorption energy of H₂O on Al surface with the equation (1) and we obtained E_{ads} = -0.266 eV.

After the determination of parameters of isolated H₂O, we studied the adsorption of this molecule on the Al surface. At the initial state, we placed the H₂O molecule on the hollow site of Al, such that the O atom is positioned above the surface plane and in the center of four Al atoms, and H(1), H(2), and O are in the same horizontal plane, meaning that the O-H(1) and O-H(2) bonds are parallel to the surface of Al(100). Figure 4 shows this configuration before and after geometry optimization.

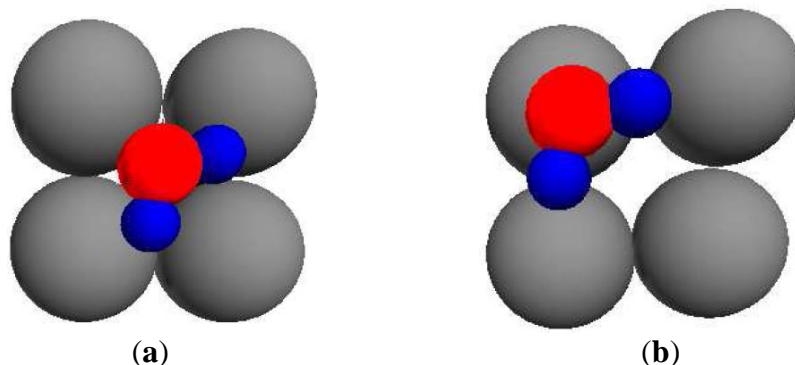


Figure 4: The figure presents a top view of the H₂O configuration adsorbed on Al(100) surface. The red spheres represent O atoms, the blue spheres the H atoms, the gray spheres the Al atoms. (a) before geometric optimization and (b) after geometry optimization.

After optimization, we observe that the H₂O molecule moves from hollow site to the nearest apical site. Regarding the geometry of the adsorbed molecule, the two O-H bonds are slightly elongated, by approximately 0.02 Å compared to their values in the free molecule. The H-O-H angle of the molecule has deviated slightly, approximately 0.5° compared to that of the free molecule. Table 2 summarizes the geometry of the free relaxed H₂O molecule and the adsorbed one.

Table 2: This table shows the geometry of the H₂O molecule in free and adsorbed states.

	H(1)-H(2) distance (Å)	O-H(1) distance (Å)	O-H(2) distance (Å)	H(1)-O-H(2) angle (°)
Free H₂O	1.548	0.978	0.978	104.51
Adsorbed H₂O	1.581	0.992	0.994	105.02

The study of structural parameters shows that the molecule in the gas phase undergoes some changes compared to its free state. Indeed, the H-O-H angle deviates slightly by 0.5° compared to that in the free state. There is also an elongation of the O-H(1) bond, ranging from 0.978 Å to 0.992 Å, and that of the O-H(2) bond, ranging from 0.978 Å to 0.994 Å. These changes indicate an interaction between the Al surface and the H₂O molecule.

3.2.2 Electronic structures

First, we analyze the local density of states of the oxygen of free and adsorbed H₂O molecule. In figure 5, we represent the densities of states of the (s + p) orbitals of the oxygen of free and adsorbed H₂O molecule, to clearly demonstrate the interaction of this molecule with the considered surface.

In this figure 5, we observe a difference between the LDOS of the adsorbed H₂O molecule's oxygen and that in the gas phase. Indeed, there is a decrease in the intensity of the peak of oxygen, especially the one located at -2.12 eV for H₂O/Al, compared to the intensity of the peak of oxygen of the isolated molecule. We also notice a displacement of about 3 eV of the LDOS of the adsorbed H₂O oxygen towards lower energies. The broadening of the peak at -6 eV can be explained by the involvement of the oxygen 2p electrons in the surface-molecule interaction. The results of the Al surface LDOS analysis are depicted in figure 6. It represents the LDOS of the aluminum p_z orbital in the clean surface and with the adsorbed H₂O molecule.

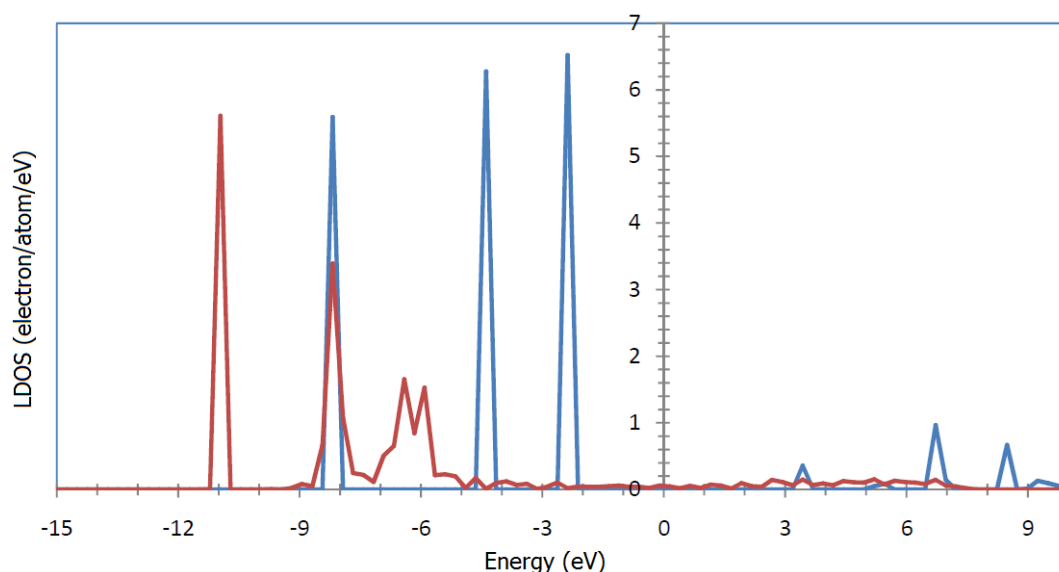


Figure 5: The figure presents the densities of states of the oxygen of free H₂O (blue curve) and adsorbed H₂O (red curve), (**eV**: Electron Volt).

In figure 6, the most remarkable feature lies between -8.5 eV and -4.5 eV. There is an increase in the intensity of the peaks of Al on the surface occupied by the molecule, compared to that of Al on the clean surface. This increase indicates the involvement of the p_z orbital electrons in the interaction with the H₂O molecule. Additionally, there is an overall decrease in intensity of the spectrum between -4 eV and +5 eV. Finally, the results of the study of the local density of states of hydrogen are shown in figure 7. Since H(1) and H(2) presented similar results for the LDOS, we present only the LDOS of one hydrogen of the adsorbed H₂O and free H₂O.

In figure 7, the remarkable difference in the LDOS of H of adsorbed H₂O compared to that in the gas phase is the shift of about 3 eV of the most intense peaks, at -8.18 eV, towards lower energies, located at -10.95 eV, indicating the stabilization of states.

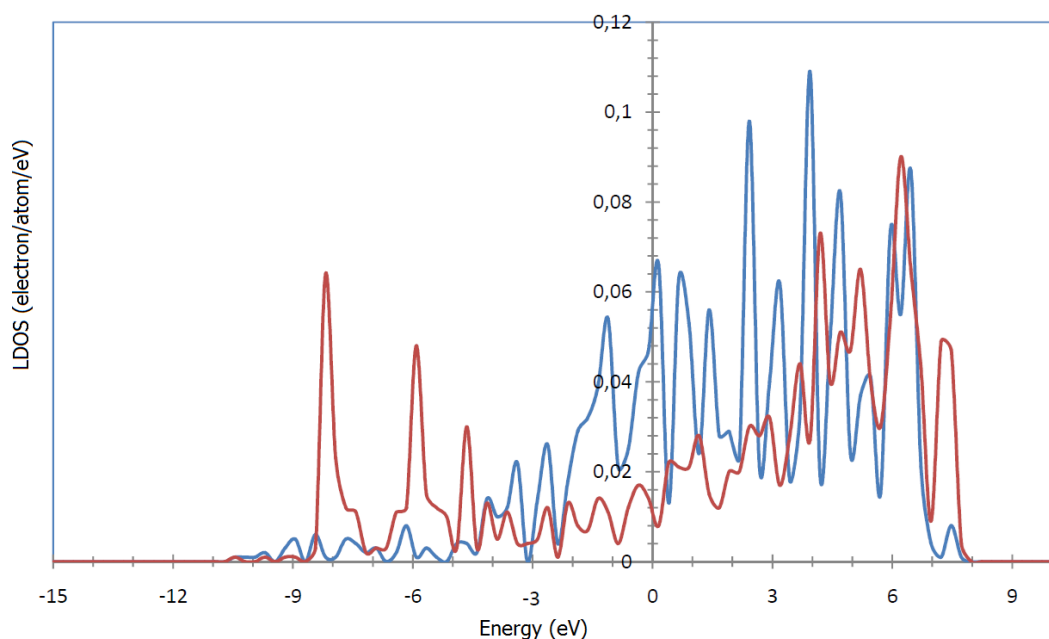


Figure 6: The figure presents the densities of states of aluminum on the clean surface (blue curve) and on the surface with the adsorbed molecule (red curve), (**eV**: Electron Volt).

From figures 5, 6 and 7, we noticed changes in the LDOS of the atoms of the adsorbed molecule compared to those of the atoms of the free molecule in the gas phase, as well as the LDOS of the occupied surface atom compared to that of the free surface atom. The most notable changes are the variation in peak intensity and the shift of the LDOS towards lower energies. These changes provide evidence of the existence of the interaction of the adsorbed H₂O molecule on the apical site of the Al(100) surface.

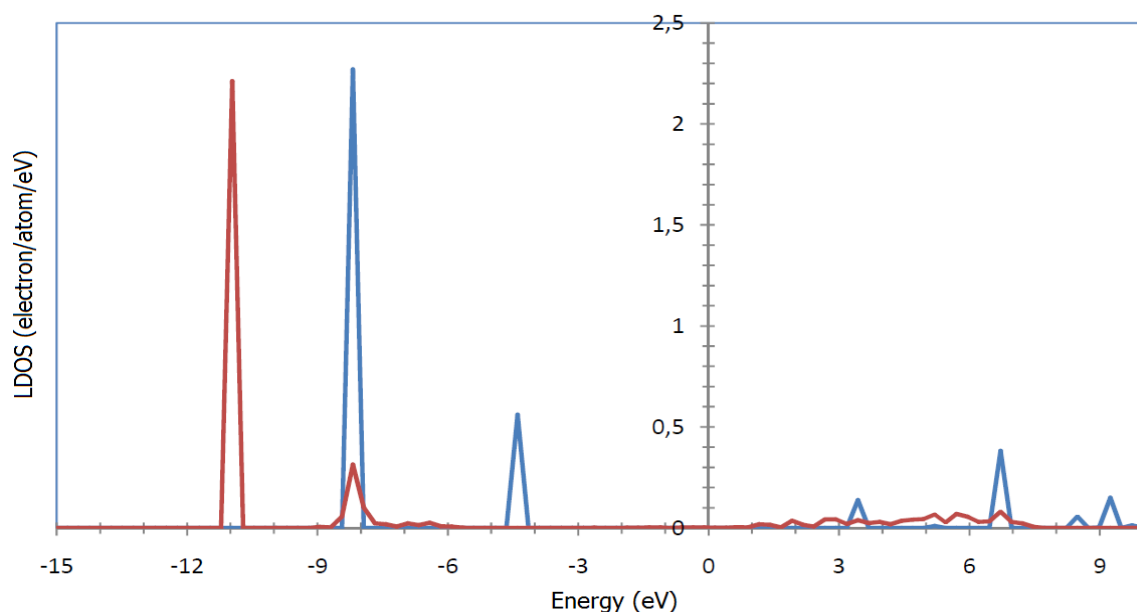


Figure 7: The figure presents the densities of states of one hydrogen of free H₂O (blue curve) and those of the adsorbed H₂O (red curve), (**eV**: Electron Volt).

3.3 Dissociated H₂O adsorption on the Al(100) Surface

3.3.1 Geometric structures and adsorption energy: Initially one H atom denoted H(1) is placed on the apical site of Al when the OH fragment is placed on other apical site. The O-H bond is parallel to the considered surface. Figure 8 illustrates this configuration.

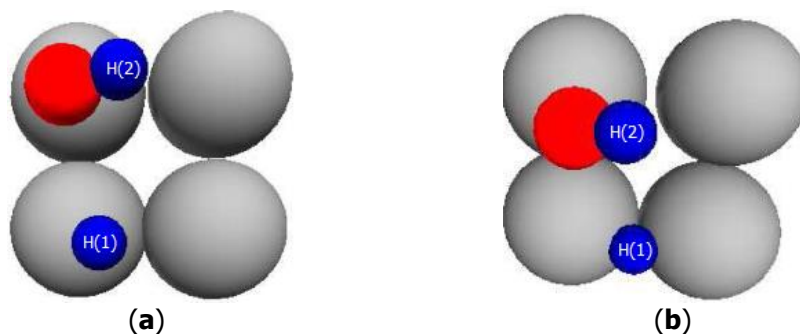


Figure 8: The figure presents a top view of coadsorbed OH and H on Al(100) surface. The red spheres represent O atoms, the blue spheres the H atoms, the gray spheres the Al atoms. (a) before geometry optimization and (b) after geometry optimization.

At the beginning of the calculation, hydrogen atom H(1) is on the apical site of Al with an Al-H distance of 1.96 Å. After geometry optimization, the H(1) atom moved towards the bridged site of the Al(100) surface to find its stable position. At this position, the distance between the H atom and the surface is 1.005 Å. For the OH fragment on the other apical site of Al, besides its displacement towards the bridged site, the important observation after geometry optimization is its inclination towards the normal to the surface, indicating its search for a stable position on the surface. The values of the structural parameters of this OH fragment are provided in table 3.

Table 3: This table presents structural parameters of OH, coadsorbed with H on the Al(100) surface, before and after geometry optimization.

	O-H distance (Å)	Al-O distance (Å)	Al-H distance (Å)	Al-O-H angle (°)
Before geometric optimization	0.978	1.900	2.000	5.64
After geometric optimization	0.979	1.720	2.170	28.69

According to table 3, the length of the adsorbed O-H bond has not changed significantly. This indicates that the O-H bond is not trending towards breaking. Regarding the Al-O distance, the reduction of 0.18 Å after adsorption explains the fact that the O atom leaves the apical site of Al and gradually moves towards the bridged site of the surface. After geometry optimization, the increase in the surface-hydrogen distance and the enlargement of the surface-O-H angle by approximately 23° indicate the deviation of the O-H bond from its initial position towards its adsorption stability position. The energy calculation results are summarized in table 4.

Table 4: This table presents calculated energies of OH and H coadsorbed on the Al(100) surface.

	$E_{(OH+H)/Al}$	E_{Al}	E_{H_2O}	E_{ads}
Energy (eV)	-1370.361	-900.126	-469.523	-0.712

According to table 4, the coadsorption energy of OH and H is -0.712 eV. This is a negative value, indicating that these two coadsorbed fragments are stable, even though their interaction with the surface is weak.

3.3.2 Electronic Structures

In figure 9, we represented the LDOS of the hydrogen atom denoted H(1) of H₂O compared to that of the coadsorbed H(1) atom with OH. H(1) is the hydrogen atom detached from water molecule as seen in figure 8. It is observed that the two peaks located at -10.95eV and -8.18eV, for the H(1) of H₂O, disappeared and replaced by a curve broadened from the energy of -9.44eV to 2.42eV, for H(1) coadsorbed with OH fragment. This indicates a mixing of H(1) orbital, which is detached from H₂O, with those of Al surface.

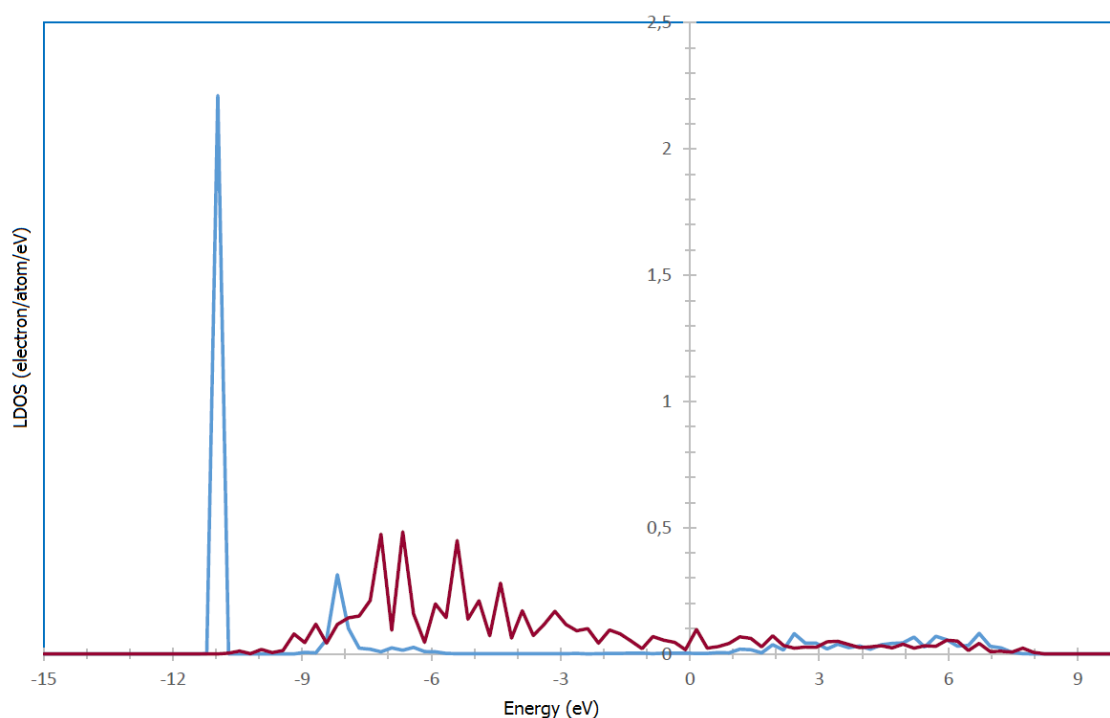


Figure 9: The figure presents the densities of states of one hydrogen of adsorbed H₂O (blue curve) and those of the hydrogen H(1) coadsorbed with OH (red curve), (eV: Electron Volt).

The figure 10 shows the densities of states of oxygen atom of the adsorbed H₂O and the oxygen of OH coadsorbed with H. We remark vanishing of the peak at -10.95eV and the shift of peaks at -6.41eV and -5.90eV towards a higher energy located at -3.63eV.

In figure 11, we see the evolution of the densities of states of the hydrogen H(2) attached to the oxygen in the case of H₂O adsorption and the OH(2) and H(1) coadsorption. We see that the peak at -10.95eV but contrary to the H(1), for which the peak at -8.18eV disappeared, those of H(2) becomes more intense. This indicates that the H(2) hydrogen remain attached to the oxygen even though the H(1) hydrogen is replaced by Al atom. From these three figures 9, 10 and 11, we observe the vanishing of peak located at -10.95eV which traduce the integrity breaking of H₂O molecule to produce two fragments which are OH and H.

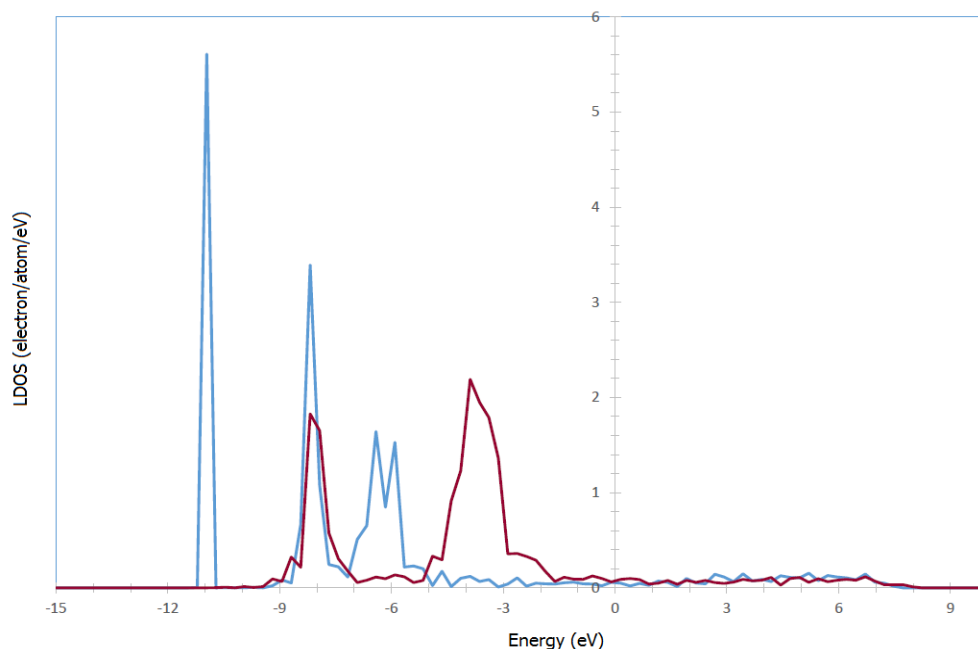


Figure 10: The figure presents the densities of states of oxygen of adsorbed H₂O (blue curve) and those of oxygen of OH fragment coadsorbed with H (red curve), (**eV**: Electron Volt).

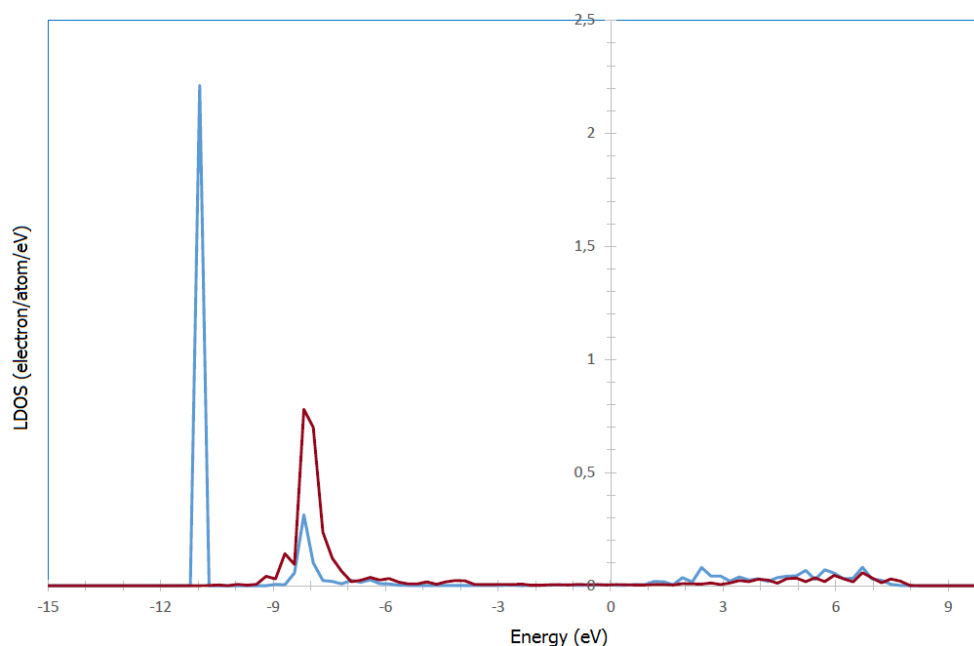


Figure 11: The figure presents the densities of states of one hydrogen of adsorbed H₂O (blue curve) and those of the hydrogen H(2) of OH fragment coadsorbed with H (red curve), (**eV**: Electron Volt).

3.4 Dissociation of H₂O molecule on Al (100) surface

In the previous sections 3.2 and 3.3, we studied the adsorption of water, hydroxide, and hydrogen species on the Al(100) surface. Investigating the coadsorption of the OH and H fragments on the surface is of great interest as it allows obtaining the final state of water molecule dissociation, i.e., the breaking of the H₂O molecule at the OH bond.

In this section, we will determine the reaction pathway for the dissociation of H₂O into molecular OH and atomic H. To do this, we use the Nudged Elastic Band (NEB) algorithm, which was introduced by Mills and Jonsson [15] in the 1990s. This method involves constructing a series of images of the system called intermediate configurations, allowing to transition from the initial to the final configuration. Forces acting on the atoms are calculated for each image. Restoring forces are established between intermediate configurations to mimic an elastic band. It allows determining the activation energy for migration, i.e., the energy required to overcome the energy barrier to transition from one stable configuration to another.

3.4.1 Reaction pathway

We considered the dissociation pathway starting from the initial state of adsorbed H₂O at the apical site of Al(100), and ending at the final state of OH and H fragments coadsorbed as described in section 3.3.

Figure 12 depicts the evolution of the system energy along the obtained pathway after optimization. Figure 13 shows the configurations of the initial I and final F states, as well as the intermediate images. The correspondence between these images and the energy is indicated in figure 12.

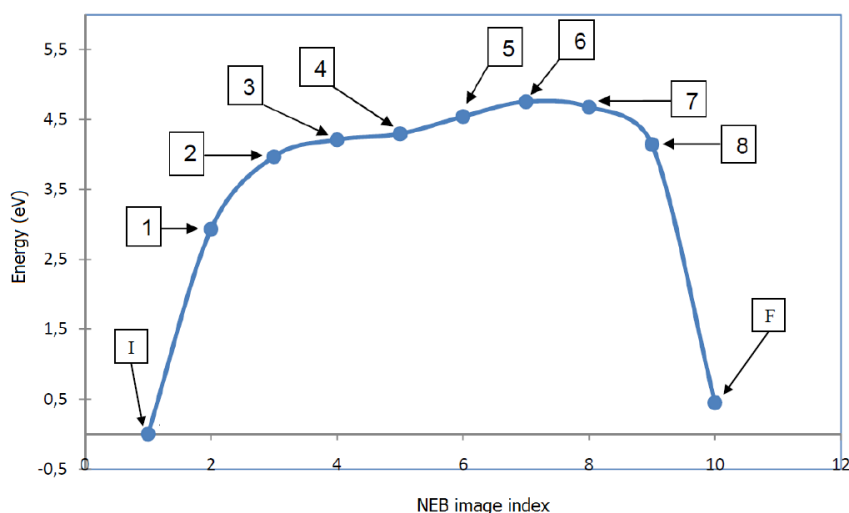


Figure 12: the figure shows the energy evolution curve of the reaction pathway for the dissociation of H₂O on Al(100).

The water molecule is adsorbed at the apical site with an oxygen pointing directly towards the surface aluminum, as showed in figure 13(I). In this situation, the adsorbate has an O-H(1) bond length equal to 0.992 Å, where H(1) is the hydrogen that will be removed in the final state, and the other bond is 0.994 Å. The oxygen is 2.250 Å from the surface of the aluminum.

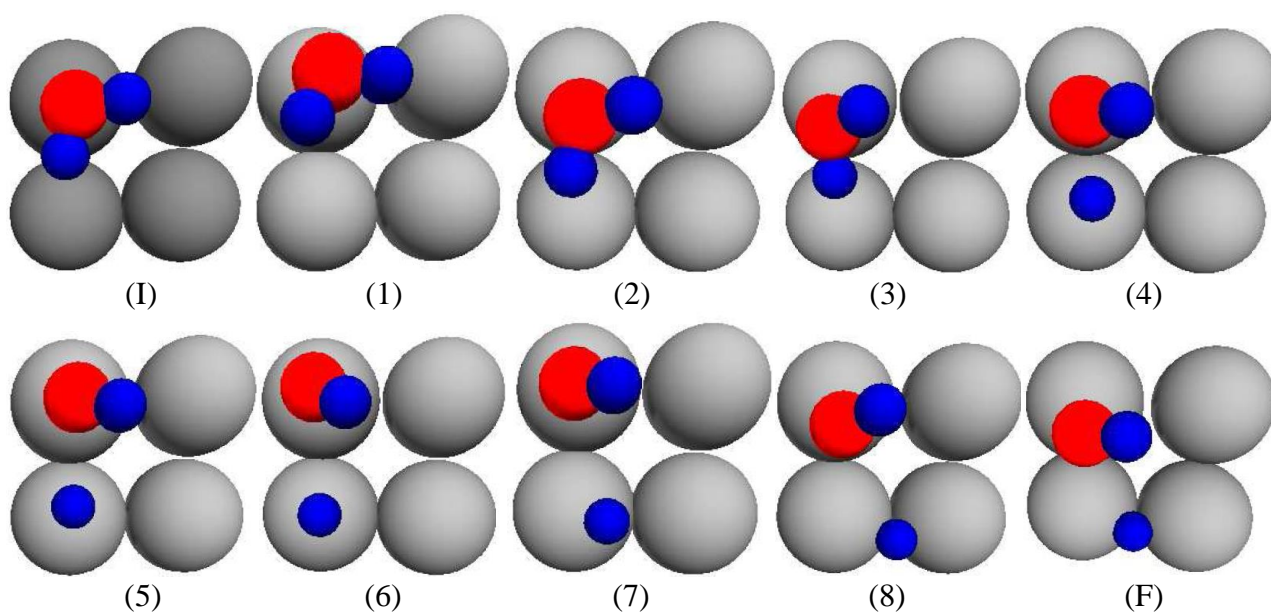


Figure 13: The figure shows the intermediate states of the reaction pathway for the dissociation of H₂O into H+OH. Small blue spheres represent hydrogens, small red spheres represent oxygens, large dark spheres represent aluminum.

Both O-H bonds are slightly modified in figure 13(1). Indeed, compared to its initial state, the bond lengths decrease by 0.006 Å for O-H(1) and 0.001 Å for O-H(2). At this state, the distance from oxygen to the upper surface of aluminum increases by about 0.37 Å compared to its initial position. In figure 13(2), the molecule has shifted from its apical position. It has mostly approached the surface, with a surface-oxygen distance of 2.321 Å instead of 2.616 Å. At the same time, the distance from oxygen to hydrogen H(1) has slightly increased, from 0.986 Å to 0.996 Å.

In figure 13(3), the molecule appears to have returned to the apical site. It has again approached the surface, reaching an Al-O distance of 1.992 Å. However, hydrogen H(1) has moved away from oxygen, resulting in an O-H(1) distance of 1.025 Å.

In this same configuration, the molecule has slightly tilted compared to the horizontal. The detachment of the H(1) atom from the water molecule begins from figure 13(4). The detached H(1) atom is located at 1.883 Å from the oxygen atom, while the length of the O-H(2) bond (H bonded to Oxygen) has slightly reduced compared to that of the initial state, as it decreases to 0.983 Å. Before reaching the transition state, in the figure 13(5), the detached H(1) atom continues to move away from the oxygen atom, while still approaching the surface of the aluminum. Indeed, the distance between H(1) and oxygen reaches 2.325 Å, and it is at a height of 1.505 Å from the surface.

The figure 13(6) corresponds to the transition state. The energy of this transition state, called the energy barrier, is maximum and is equal to 4.754 eV. The geometric parameters of this state will be given in the following section 3.4.2. Once this energy barrier is reached, the system seeks to stabilize by minimizing its energy.

In figure 13(7), the atomic hydrogen and the OH fragment move further apart. In fact, this movement is due to the repulsion between the two species. The distances O-H(1), Al-O, and Al-H(1) are 2.878 Å, 1.791 Å, and 1.404 Å respectively. It is observed in the penultimate image that the hydrogen H(1) and the OH molecule have almost returned to their stabilizing sites, thus being at a distance of 1.085 Å for Al-H(1) and 1.724 Å for Al-O.

In the last image, figure 13(F), the two fragments, with their energies decreased, stabilize. The OH molecule finds its equilibrium by orienting its hydrogen at 28.69° with respect to the surface horizontal, while the hydrogen lands on the bridging site, finding its equilibrium at distances O-H(1) equal to 2.994 Å and Al-H(1) equal to 1.005 Å. The distances of the water molecule atoms from the upper surface of aluminum, as well as the lengths of the two O-H bonds, for each intermediate image of the reaction pathway, are summarized in table 5.

Table 5: this table summarizes different bond lengths and distances on the NEB method reaction pathway.

Images	O-H(1) (Å)	O-H(2) (Å)	Al-O (Å)	Al-H(1) (Å)	Al-H(2) (Å)
Initial (I)	0.992	0.994	2.250	2.372	2.302
(1)	0.986	0.993	2.616	2.982	2.685
(2)	0.996	0.995	2.321	2.627	2.593
(3)	1.025	0.996	1.992	1.936	2.455
(4)	1.883	0.983	1.870	1.551	2.404
(5)	2.325	0.981	1.883	1.505	2.375
(6)	2.719	0.979	1.848	1.634	2.394
(7)	2.878	0.976	1.791	1.404	2.340
(8)	3.090	0.985	1.724	1.085	2.339
Final (F)	2.994	0.979	1.723	1.005	2.170

3.4.2 Transition state

The transition state is the highest energy point of the reaction pathway. The transition state is located at the 6th intermediate image, in figure 13(6). In this transition state, the oxygen and H(2) atoms of the OH fragment remain bonded with an O-H bond length of 0.979 Å. This bond length is very close to that of free OH, which is found to be 0.978 Å. The inclination angle of this molecule with respect to the flat surface of aluminum is 33.91°. The hydrogen H(1) detached from the water molecule is located at 1.634 Å from the flat surface of Al(100), where the distance between this atom and the oxygen atom extends up to 2.719 Å. The oxygen is 1.848 Å above the surface. The transition state corresponds to an activation energy of 4.754 eV.

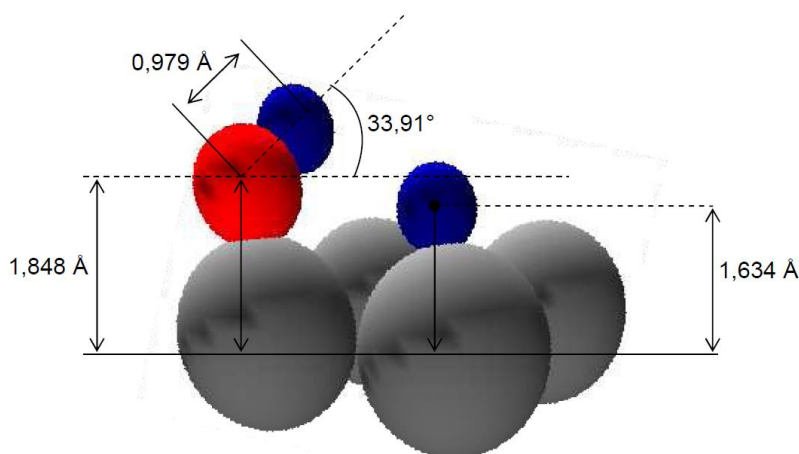


Figure 14: The figure shows the profile view of the geometry of the transition state of the reaction pathway.

4. CONCLUSION

This work focuses on the study of the adsorption and dissociation of the water molecule on aluminum surface. This water molecule, the most abundant in nature, is the largest source of hydrogen after its dissociation. Aluminum, a widely available metal on the Earth's crust, is chosen for its catalytic properties.

We used the DACAPO code for all calculations. DACAPO is an ab initio code based on density functional theory (DFT) in its pseudopotential version, where wave functions are developed on a plane wave basis. Simulations with the DACAPO program allowed us to determine numerous characteristic parameters of the system, such as the lattice parameter for aluminum, the lengths of the O-H bonds, and the measurement of the HOH angle for the H₂O molecule. The adsorption energy of the water molecule on the apical site of the (100) surface of aluminum was calculated. The negative value of this energy indicates the interaction of the molecule with the surface, and its relatively lower absolute value explains that we are dealing with physisorption.

The coadsorption of hydroxide and hydrogen was studied, initially on the apical site of the Al(100) surface, but the two species moved to bridged sites after geometric optimization. This step was taken to identify the final configuration of water molecule dissociation. The co-adsorption energy of the two species showed that the dissociatively adsorbed water molecule is more stable on the Al(100) surface than the molecularly adsorbed one. Thus, it is possible to dissociate the water molecule on the surface of aluminum.

The process of dissociating the water molecule on Al(100) was studied using the NEB method. We explored the lowest energy dissociation pathway, considering the adsorbed water molecule on the apical site of Al(100) as the initial configuration and the OH fragment and the co-adsorbed H atom as the final configuration. The energy barrier of dissociation was revealed at the transition state, and its relatively high value suggested that it is preferable to use aluminum in the form of alloys and explore other reaction pathways.

In this work, we only investigated a single dissociation pathway of the water molecule. Indeed, we considered only the apical site for the initial and bridged site for the final configurations of the pathway. Thus, it is possible to establish a range characterizing dissociation pathways by considering other adsorption sites. This approach could be extended to other metals and/or other molecules.

List of acronyms:

BFGS: Broyden-Fletcher-Goldfarb-Shanno algorithm;
DACAPO: Danish Ab Initio Pseudopotential Code;
DFT: Density Functional Theory;
GGA: Generalized Gradient Approximation;
LDOS: Local Density Of State;
NEB: Nudged Elastic Band.

5. REFERENCES

1. Armor JN. New catalytic technology commercialized in the USA during the 1980's. *Appl Catal.* 1991;78(2):141-73.
2. Armor JN. New catalytic technology commercialized in the USA during the 1990's. *Appl Catal A.* 2001;222(1-2):407-26.
3. Kayser H. Über die Verdichtung von Gasen an Oberflächen in ihrer Abhängigkeit von Druck und Temperatur. *Ann Phys Chem.* 1881;248(4):526-37. Available from: <https://doi.org/10.1002/andp.18812480404>
4. Harder S. From Limestone to Catalysis: Application of Calcium Compounds as Homogeneous Catalysts. *Chem Rev.* 2010;110(7):3852-76. Available from: <https://pubs.acs.org/doi/10.1021/cr9003659>
5. Hammer B, Hansen LB, Nørskov JK. Improved adsorption energetics within density-functional theory using revised Perdew-Burke-Ernzerhof functionals. *Phys Rev B.* 1999;59(11):7413-21.
6. Ab initio pseudopotential code Dacapo (version 2.7.3, 2003), developed at CAMPOS. Center for Atomic-Scale Materials Physics, Department of Physics, Technical University of Denmark, Lyngby; see <http://www.fysik.dtu.dk> for details.
7. Vanderbilt D. Soft self-consistent pseudopotentials in a generalized eigenvalue formalism. *Phys Rev B.* 1990;41(11):7892-5.
8. Perdew JP, Wang Y. Accurate and simple analytic representation of the electron-gas correlation energy. *Phys Rev B.* 1992;45(23):13244-9.
9. Perdew JP, Chevary JA, Vosko SH, Jackson KA, Pederson MR, Singh DJ, et al. Atoms, molecules, solids, and surfaces: Applications of the generalized gradient approximation for exchange and correlation. *Phys Rev B.* 1992;46(11):6671-87.
10. Feynman RP. Forces in Molecules. *Phys Rev.* 1939;56(4):340-3.
11. Monkhorst HJ, Pack JD. Special points for Brillouin-zone integrations. *Phys Rev B.* 1976;13(12):5188-92.
12. Baraldi A, Lizzit S, Comelli G, Kiskinova M, Rosei R, Honkala K, et al. Spectroscopic Link between Adsorption Site Occupation and Local Surface Chemical Reactivity. *Phys Rev Lett.* 2004;93(4):046101-1-4.
13. Haroun MF. Simulation numérique de l'activation du méthane sur la surface (111) du nickel idéale et avec un ad atome [Doctoral thesis]. Strasbourg: University Louis Pasteur, Strasbourg I; 2007.
14. Moussounda PS. Adsorption et Activation du Méthane et du Méthanol sur la surface (100) du Pt: une étude par la fonctionnelle de la densité [Doctoral thesis]. Strasbourg: University Louis Pasteur, Strasbourg I; 2006.
15. Mills G, Jonsson H. Quantum and thermal effects in H₂ dissociative adsorption: Evaluation of free energy barriers in multidimensional quantum systems. *Phys Rev Lett.* 1994;72(7):1124-7.
16. Witt W. Absolute Präzisionsbestimmung von Gitterkonstanten an Germanium und Aluminium-Einkristallen mit Elektroneninterferenzen. *Z Naturforsch A.* 1967;22a:92-5. Available from: <https://doi.org/10.1515/zna-1967-0115>
17. Hoy AR, Bunker PR. A Precise Solution of the Rotation-Bending Schrödinger Equation for a Triatomic Molecule with Application to the Water Molecule. *J Mol Spectrosc.* 1979;74(1):1-8.

18. Materzanini G, Tantardini GF, Lindan PJD, Saalfrank P. Water adsorption at metal surfaces: A first principles study of the $\sqrt{3}\times\sqrt{3}$ R30°H₂O bilayer on Ru(0001). *Phys Rev B*. 2005;71(15):155414-1-17.
19. Xantheas SS, Dunning TH. Ab initio studies of cyclic water clusters (H₂O)_n, n=1-6. I. Optimal structures and vibrational spectra. *J Chem Phys*. 1993;99(11):8774-92.
20. Rakotoveloa G. Etat de surface réel de BaTiO₃ dans un contexte réactif [Doctoral thesis]. Strasbourg: University Louis Pasteur, Strasbourg I; 2008.



How to cite this article: Dimbimalala Randrianasoloharisoa, Herimanampisoa Randrianarinjaka, and Georgette Ramanantsizehena. Theoretical Study of Water Dissociation on Aluminum (100) Surface using Density Functional Theory. *Am. J. innov. res. appl. sci.* 2024; 19(2): 57-68 Doi: 10.5281/zenodo.13354320

This is an Open Access article distributed in accordance with the Creative Commons Attribution Non Commercial (CC BY-NC 4.0) license, which permits others to distribute, remix, adapt, build upon this work non-commercially, and license their derivative works on different terms, provided the original work is properly cited and the use is non-commercial. See:

<http://creativecommons.org/licenses/by-nc/4.0/>